

This article was downloaded by:

On: 25 January 2011

Access details: *Access Details: Free Access*

Publisher *Taylor & Francis*

Informa Ltd Registered in England and Wales Registered Number: 1072954 Registered office: Mortimer House, 37-41 Mortimer Street, London W1T 3JH, UK



## Separation Science and Technology

Publication details, including instructions for authors and subscription information:

<http://www.informaworld.com/smpp/title~content=t713708471>

### Productivity Considerations and Design Charts for Biomolecule Capture with Periodic Countercurrent Adsorption Systems

Giorgio Carta<sup>a</sup>; Ernie X. Perez-Almodovar<sup>a</sup>

<sup>a</sup> Department of Chemical Engineering, University of Virginia, Charlottesville, VA, USA

Online publication date: 21 January 2010

**To cite this Article** Carta, Giorgio and Perez-Almodovar, Ernie X.(2010) 'Productivity Considerations and Design Charts for Biomolecule Capture with Periodic Countercurrent Adsorption Systems', *Separation Science and Technology*, 45: 2, 149 — 154

**To link to this Article:** DOI: 10.1080/01496390903423865

URL: <http://dx.doi.org/10.1080/01496390903423865>

## PLEASE SCROLL DOWN FOR ARTICLE

Full terms and conditions of use: <http://www.informaworld.com/terms-and-conditions-of-access.pdf>

This article may be used for research, teaching and private study purposes. Any substantial or systematic reproduction, re-distribution, re-selling, loan or sub-licensing, systematic supply or distribution in any form to anyone is expressly forbidden.

The publisher does not give any warranty express or implied or make any representation that the contents will be complete or accurate or up to date. The accuracy of any instructions, formulae and drug doses should be independently verified with primary sources. The publisher shall not be liable for any loss, actions, claims, proceedings, demand or costs or damages whatsoever or howsoever caused arising directly or indirectly in connection with or arising out of the use of this material.

# Productivity Considerations and Design Charts for Biomolecule Capture with Periodic Countercurrent Adsorption Systems

Giorgio Carta and Ernie X. Perez-Almodovar

Department of Chemical Engineering, University of Virginia, Charlottesville, VA, USA

**General design charts are presented to enable the prediction of the steady state performance of periodic countercurrent adsorption systems for conditions typical of biomolecule capture on selective adsorbents. The underlying model assumes that the process is controlled by diffusion in the intraparticle macropores and that the adsorption equilibrium can be described by the Langmuir isotherm. Model results are presented in dimensionless form for isotherms ranging from highly favorable to nearly linear. When the isotherm is highly favorable, operating with 2 to 3 columns in series reduces the amount of adsorbent needed by 15 to 35% when the process is operated with a rapid cycle. Smaller improvements are predicted for longer cycles, while larger improvements are predicted when the isotherm is less favorable. Increasing the number of columns in series beyond 2 or 3 is probably unwarranted since incremental improvements decline rapidly going from 2 to 3 columns. Use of the charts is illustrated with a specific example of application to a protein A capture system.**

**Keywords** adsorption; capture; biomolecules; affinity; multi-column systems

## INTRODUCTION

Periodic countercurrent (PCC) adsorption systems are used extensively in ion exchange and water purification systems for the removal of trace contaminants. In these applications, the adsorption isotherm is often nearly linear. As a result, the mass transfer zone is very broad and the breakthrough curve for a single column operation is very shallow, resulting in a poor utilization of the adsorption capacity. In these cases, PCC systems, such that illustrated in Fig. 1, can be used to improve process efficiency (1). These systems simulate a true countercurrent operation by switching multiple fixed-bed columns at periodic time intervals in a merry-go-round arrangement. Just a few columns in series normally provide a close approach to the behavior of an ideal countercurrent process, but without the complexities of actually moving individual particles against a countercurrently moving fluid. The switching

can be obtained with a suitable system of valves so that ordinary fixed-bed columns can be used.

The advantages of PCC adsorption are well established for conditions where the adsorption isotherm is linear or nearly linear and detailed analyses have been published for these cases based on model simulations (e.g., refs (2–5)) and on experiments (e.g., ref (6)). Besides trace contaminant removal there has also been interest in applying PCC approaches to the adsorptive capture of biomolecules (7–8). Arve and Liapis (8), for example, discussed a PCC system for biospecific adsorption and showed by numerical simulation that subdividing a single fixed bed in two could improve substantially the utilization of adsorption capacity but only for very short beds. More recently, other authors (9) have described equipment to implement PCC adsorption for protein capture in a biopharmaceutical manufacturing environment.

An important consideration in assessing the potential advantages of PCC systems for biomolecule capture applications is that the isotherm in bioadsorption is usually highly favorable, which results in relatively narrow mass transfer zones. As a result, the advantages of PCC adsorption over simpler one-column systems will depend strongly on the specific characteristics of the adsorbent and the operating conditions. Thus, in practice, detailed computer simulations or extensive experimentation will be needed to determine potential improvements. In order to simplify this task, this paper provides simple dimensionless design charts that can be used to assess potential advantages of PCC operations without having to resort to detailed computer simulations. The charts are also useful for preliminary design of optimum capture systems and complement previously published work that was either limited to the linear isotherm case (3,5) or based on approximate calculations for a saturation or irreversible isotherm (2).

## MATHEMATICAL MODEL

The key assumptions made in the mathematical model used in this work are as follows:

1. Plug flow without axial dispersion;
2. Intraparticle mass transfer controlled by pore diffusion with negligible boundary layer mass transfer resistance;

Received 30 June 2009; accepted 30 September 2009.

Address correspondence to Giorgio Carta, Department of Chemical Engineering, University of Virginia, 102 Engineers' Way, Charlottesville, Virginia, USA. E-mail: gc@virginia.edu

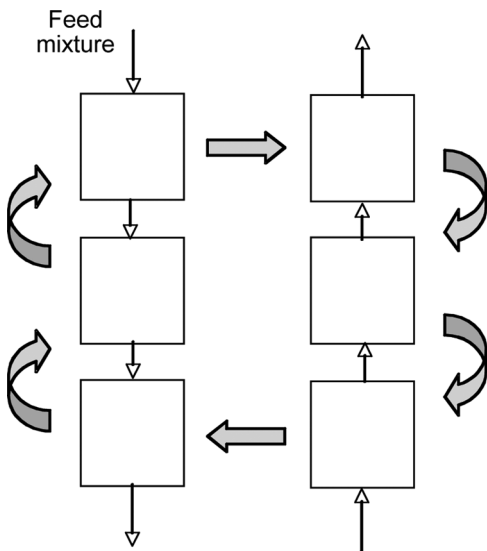


FIG. 1. Periodic countercurrent adsorption system. The individual columns are switched in position at periodic time intervals as indicated by the arrows. Note that each adsorption column spends equal time in the adsorption train (left) and in the desorption/regeneration train (right).

3. Local equilibrium between adsorbed and pore fluid concentrations; and
4. Adsorption equilibrium described by Langmuir or constant-separation-factor isotherm.

These assumptions are quite reasonable for protein adsorption on stationary phases designed for industrial scale applications. The first assumption is justified by the fact that the reduced velocity,  $v' = v d_p / D_0$ , is usually greater than several hundreds in these applications (10). As a result at the c-term in the van Deemter equation and, hence, adsorption kinetics, is dominant as long as column packing is reasonably uniform and the hardware is well designed. The second assumption is justified for most open-pore adsorbents, such as those used for biospecific or affinity adsorption. In these cases, the Biot number,  $Bi = k_f r_p / D_e$ , which measures the relative importance of intraparticle and external mass transfer, is usually very large, so that the boundary layer resistance is negligible (11). The third assumption is valid for most practical cases involving ion exchange or hydrophobic binding. However, even for biospecific adsorption, where the binding kinetics can be limiting in certain cases, the time constants for the formation of the ligand-protein bond are usually much smaller than diffusion times in porous particles so that local equilibrium prevails at each point within the particle. Finally, the last assumption is only a mathematical approximation. Obviously, the basic tenets of the Langmuir model (single site binding with no lateral interactions of the adsorbed molecules) are not met in reality by many protein adsorption systems. Nevertheless, the Langmuir model has been shown to be adequate for an accurate, albeit empirical,

description of protein adsorption equilibrium in systems as diverse as ion exchange, hydrophobic interaction, and biospecific adsorption (e.g., see ref (12)).

Based on the above assumptions, the following equations and boundary conditions can be used to describe the adsorption train of a PCC system:

$$\varepsilon \frac{\partial C}{\partial t} + (1 - \varepsilon) \frac{\partial \bar{q}}{\partial t} + u \frac{\partial C}{\partial z} = 0 \quad (1)$$

$$z = 0, \quad C = C_F \quad (1a)$$

$$\varepsilon_p \frac{\partial c}{\partial t} + \frac{\partial q}{\partial t} = \frac{D_e}{r^2} \frac{\partial}{\partial r} \left( r^2 \frac{\partial c}{\partial r} \right) \quad (2)$$

$$r = 0, \quad \frac{\partial c}{\partial r} = 0 \quad (2a)$$

$$r = r_p, \quad c = C \quad (2b)$$

$$q = \frac{q_m b c}{1 + b c} \quad (3)$$

where the average protein concentration in the particle,  $\bar{q}$ , given by:

$$\bar{q} = \frac{3}{r_p^3} \int_0^{r_p} (\varepsilon_p c + q) r^2 dr \quad (4)$$

includes both adsorbed molecules as well as those that are present in the intraparticle macropores. Because of assumptions 3 and 4, combining Eqs. 2 and 3 yields the following result:

$$\frac{\partial c}{\partial t} = \frac{D_e}{\varepsilon_p + \frac{q_m b}{(1+b c)^2}} \frac{1}{r^2} \frac{\partial}{\partial r} \left( r^2 \frac{\partial c}{\partial r} \right) \quad (5)$$

in place of Eq. 2. In principle, analogous equations can be written to describe the desorption train. In practice, however, in bioprocess applications, the isotherm is extremely sensitive to the mobile phase composition. As a result, while the adsorption isotherm is generally quite favorable for the load step, conditions are usually such that essentially no binding occurs during elution. In this case, elution is completely diffusion limited and fast because of the high concentration driving force. Furthermore, clean-in-place operations are often needed and these are generally dependent only on the time of exposure of the particles to the sanitizing agent. The net result is that the time each adsorbent particle must spend in the desorption/regeneration train is approximately independent of the number of column sections or their length. Thus, we can assume that the switch time is given by:

$$t_{switch} = \frac{t_{reg}}{N_c} \quad (6)$$

where  $t_{reg}$  is the time each particle must spend in the desorption/regeneration train and  $N_c$  is the number of columns in series, which is assumed to be the same for the adsorption and the desorption trains. Accordingly, the total cycle time, required for a column to go through the adsorption or the desorption train is  $t_{cycle} = N_c t_{switch} = t_{reg}$ . When this time is sufficient, a clean adsorbent bed is available at each switch so that only the loading columns need to be simulated. If we consider, for example, a system with 4 total columns (2 in the adsorption train and 2 in the desorption train), the total time spent by each particle in each train will be  $t_{reg}$ , while the switch time will be  $t_{reg}/2$ . Obviously, a different number of columns can be used in the adsorption and desorption trains. For instance, if only 1 column is used in the regeneration train, then the switch time must be equal to  $t_{reg}$  or greater regardless of the number of columns in series in the adsorption train.

The dimensionless form of Eqs. 1–5 is given by the following equations:

$$\frac{\varepsilon}{\Lambda} \frac{\partial X}{\partial \tau} + \frac{\partial \bar{Y}}{\partial \tau} + \frac{\partial X}{\partial \zeta} = 0 \quad (7)$$

$$\zeta = 0, X = 1 \quad (7a)$$

$$\frac{\partial x}{\partial \tau} = \frac{n f(x)}{15 \rho^2} \frac{\partial}{\partial \rho} \left( \rho^2 \frac{\partial x}{\partial \rho} \right) \quad (8)$$

$$\rho = 0, \quad \frac{\partial x}{\partial \rho} = 0 \quad (8a)$$

$$\rho = 1, \quad x = X \quad (8b)$$

where the dimensionless variables are defined as follows:

$$X = \frac{C}{C_F} \quad (9)$$

$$\bar{Y} = \frac{\bar{q}}{q_F} \quad (10)$$

$$x = \frac{c}{C_F} \quad (11)$$

$$\Lambda = \frac{(1 - \varepsilon)q_F}{C_F} \quad (12)$$

$$\tau = \frac{1}{\Lambda L} \frac{ut}{L} \quad (13)$$

$$\zeta = \frac{z}{L} \quad (14)$$

$$\rho = \frac{r}{r_p} \quad (15)$$

$$f(x) = \frac{\frac{\varepsilon_p}{q_m b} + \frac{1}{R}}{\frac{\varepsilon_p}{q_m b} + \frac{1}{(1 + \frac{1 - R}{R}x)^2}} \quad (16)$$

$$n = \frac{15(1 - \varepsilon)D_e L}{r_p^2 \mu} \quad (17)$$

$$R = \frac{1}{1 + b C_F} \quad (18)$$

A numerical solution is required and was obtained by discretizing both the particle radial coordinate and the column axial coordinate by finite differences, the latter with a backwards scheme. The resulting ordinary differential equations were then integrated for a given switch period using subroutine DIVPAG of the International Mathematical and Statistical Library (IMSL), which uses Gear's method for stiff systems of ordinary differential equations. In order to simulate the PCC switching of columns, at the end of each period,  $x$  and  $X$  values were reassigned according to Fig. 1 and the numerical integration repeated until reaching a periodic state. Calculations were done with a number of discretization points sufficiently large that their actual values did not affect the numerical results. For a most difficult case, corresponding to  $R = 0.01$ , we used 50 axial and 39 radial discretization points. For each case, the cyclic calculation was repeated until the maximum effluent concentration at the outlet from the adsorption train was within 0.1% of the value found in the previous cycle.

In dimensionless form, the model parameters are the total number of transfer units,  $n$ , the dimensionless total cycle time  $\tau_p = ut_{cycle}/\Lambda L = uN_c t_{switch}/\Lambda L$ , the isotherm parameter,  $R$ , the number of column sections in series,  $N_c$ , and the ratios  $\varepsilon/\Lambda$  and  $\varepsilon_p/q_m b$ . However, in practice, these two ratios are usually quite small and can be neglected for high-capacity adsorbents with favorable isotherms and dilute solutions, where the partition ratio,  $\Lambda$ , and the initial isotherm slope,  $q_m b$ , are both large. For these conditions, a general result can be found by setting a maximum outlet concentration at  $\zeta = 1$  and calculating the number of transfer units required using different numbers of columns in series over a range of values of  $n\tau_p = 15(1 - \varepsilon)D_e t_{cycle}/\Lambda r_p^2$ . The product  $n\tau_p$  is independent of residence time and can be estimated knowing the adsorbent capacity, the particle size, the effective diffusivity, and the time required for desorption and regeneration of the adsorbent particles by taking  $t_{cycle} = t_{reg}$ .

## RESULTS AND DISCUSSION

Numerical results were obtained using typical values of  $\varepsilon = 0.35$  and  $\varepsilon_p = 0.5$  for  $R = 0.01, 0.1, 0.2$ , and  $0.9$ . The two smaller values of  $R$  correspond to nearly rectangular,

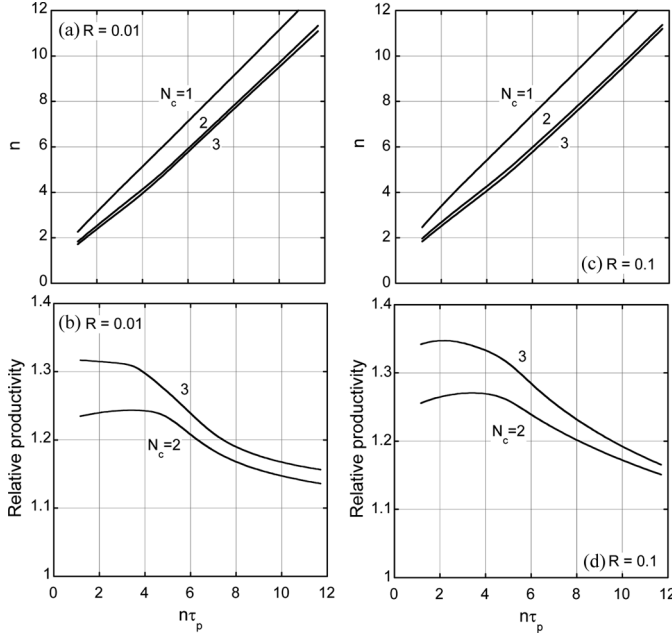


FIG. 2. Total number of transfer units required for  $X_{out} \leq 0.1$  (top) and relative productivity (bottom) with different number of column sections in series.  $R = 0.01$  for a and b;  $R = 0.1$  for c and d.

highly-favorable isotherms, while the largest one corresponds to a nearly linear isotherm. Although unlikely to be found in actual biomolecule capture systems, this case is included for comparison purposes. Results for  $\Lambda = 10$  are given in Figs. 2 and 3 for  $X_{out} \leq 0.1$  in the periodic state

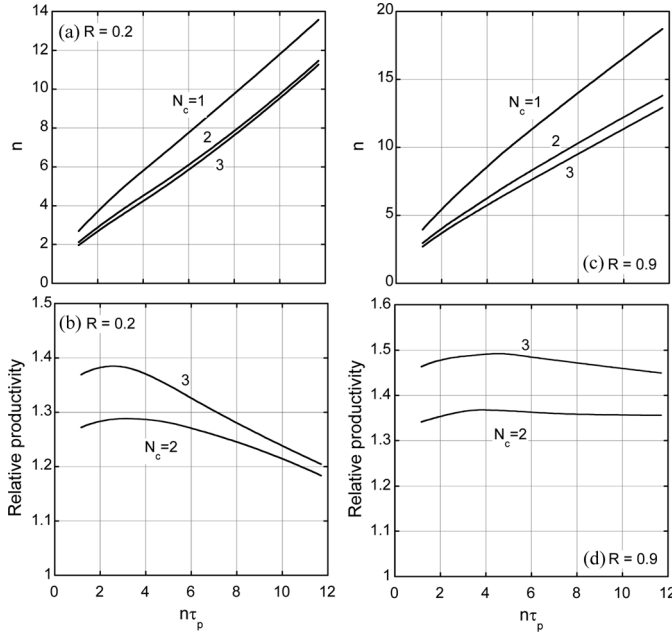


FIG. 3. Total number of transfer units required for  $X_{out} \leq 0.1$  (top) and relative productivity (bottom) with different number of column sections in series.  $R = 0.2$  for a and b;  $R = 0.9$  for c and d.

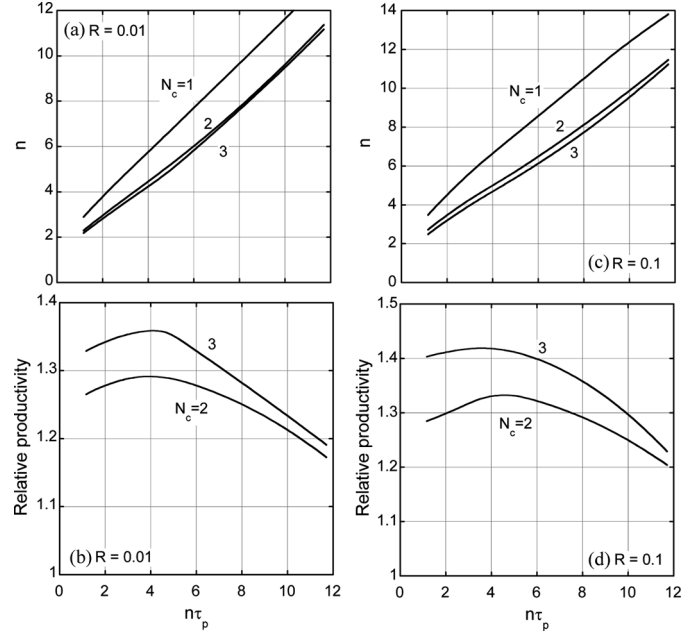


FIG. 4. Total number of transfer units required for  $X_{out} \leq 0.01$  (top) and relative productivity (bottom) with different number of column sections in series.  $R = 0.01$  for a and b;  $R = 0.1$  for c and d.

with one, two, or three column sections in series. The corresponding results for  $X_{out} \leq 0.01$  are given in Figs. 4 and 5. In both cases, the relative productivity is calculated as the ratio  $n|_{N_c}/n|_{N_c=1}$  at the same value of the dimensionless switch period  $n\tau_p$ . For these conditions the effects of  $\varepsilon/\Lambda$

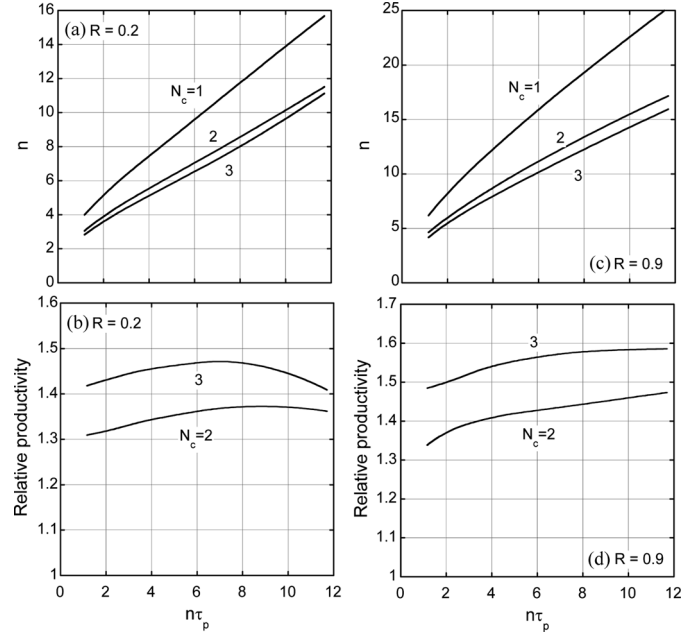


FIG. 5. Total number of transfer units required for  $X_{out} \leq 0.01$  (top) and relative productivity (bottom) with different number of column sections in series.  $R = 0.2$  for a and b;  $R = 0.9$  for c and d.

and  $\varepsilon_p/q_m b$  are negligible, so that the same curves can also be used for larger values of  $\Lambda$ . For  $R=0.01$  and  $X_{out} \leq 0.1$ , the numerical solution for  $N_c=1$  is practically indistinguishable from the result for the irreversible isotherm limit ( $R=0$ ) predicted by the analytical solution of Cooper and Liberman (13). The latter is approximated by the following equation valid for  $n > 2.5$  (10):

$$n = 1.03 + n\tau_p \quad (19)$$

Increasing the number of column sections from  $N_c=1$  to 2 is seen to reduce  $n$ , and thus, the total column length, and to increase productivity by a maximum of about 24%. However, the relative effect becomes increasingly less pronounced as  $n\tau_p$  is increased. Moreover, increasing  $N_c$  further has only a small incremental effect, suggesting that subdividing the column in more than two sections would likely be unjustified.

The results for lower values of  $R$  shown in Fig. 3 mimic those in Fig. 2. The main difference is that as  $R$  is increased and the adsorption isotherm becomes less favorable, the relative productivity becomes somewhat less dependent on  $n\tau_p$  but also more greatly influenced by  $N_c$ . Even with  $R=0.9$ , however, the maximum improvement in productivity is only about 35% when  $N_c=2$ .

The results for  $X_{out} \leq 0.01$  shown in Figs. 4 and 5 exhibit similar trends. The improvement with  $N_c$  is very similar in magnitude to the case of  $X_{out} \leq 0.1$  when  $R$  is small, since the breakthrough curve is relatively sharp and there is not much difference in the times at which values of  $X_{out}=0.1$  and  $X_{out}=0.01$  are reached. However, the improvement is more pronounced and the maximum shifts to higher  $n\tau_p$ -values when  $R$  is larger and the isotherm closer to linearity.

## APPLICATION EXAMPLE

The capture of IgG from a 1-mg/cm<sup>3</sup> solution on the protein A adsorbent UNOsphere SUPrA (Bio-Rad Laboratories, Hercules, CA, USA) is used as an example. The relevant properties determined by Perez-Almodovar (14) are summarized in Table 1. We assume  $t_{cycle}=t_{reg}=1,800$  s and  $X_{out} \leq 0.1$ . The following values of the dimensionless parameters are obtained:

$$\Lambda = 24.4$$

$$\frac{\varepsilon}{\Lambda} = 0.0143$$

$$\frac{\varepsilon_p}{q_m b} = 0.000227$$

$$R = 0.0137$$

$$n\tau_p = 5.31$$

TABLE 1  
Parameter values for IgG capture on UNOsphere SUPrA (Perez-Almodovar (14))

Parameter	Value	Units
$d_p$	57	μm
$\varepsilon$	0.35	
$\varepsilon_p$	0.62	
$q_m$	38	mg/cm <sup>3</sup> particle
$b$	72	cm <sup>3</sup> /mg
$D_e$	$6.0 \times 10^{-8}$	cm <sup>2</sup> /s

For these conditions, interpolating between the values read from Fig. 2a and 2b, we obtain  $n=6.5$ , 5.3, and 5.1, using  $N_c=1$ , 2, and 3, respectively. For a comparison, detailed simulations for the actual parameter values yield  $n=6.61$ , 5.30, and 5.11, for  $N_c=1$ , 2, and 3, respectively, practically indistinguishable from the values read from the figures. Note that in either case, the corresponding column lengths can be found if a superficial velocity is selected. At 600 cm/h ( $u=0.167$  cm/s), we obtain one column with  $L=15$  cm, two columns each 6.1 cm long, or three columns each 4.0 cm long. It should be noted that, in practice, there can be technological and procedural limitations to packing reliably and validating large diameter columns with very short bed heights. Clearly, such limitations need to be taken into account in the design of actual systems.

## CONCLUSIONS

The charts provided in this paper allow rapid predictions of the periodic state performance of a PCC adsorptive process for conditions that are typically found in biochromatographic capture steps. Although the charts are provided only for a few different values of the dimensionless parameters, interpolation between values provides reasonably accurate predictions for practical cases using basic parameters describing the adsorption isotherm and the intraparticle pore diffusivity. The switching time is determined independently either experimentally or from models based on the time required to completely desorb and clean the adsorbent particles.

## NOTATION

$b$	parameter in Langmuir isotherm (cm <sup>3</sup> /mg)
$c$	concentration in pore fluid (mg/cm <sup>3</sup> )
$C$	concentration in external fluid (mg/cm <sup>3</sup> )
$C_F$	feed concentration (mg/cm <sup>3</sup> )
$D_e$	effective intraparticle diffusivity (cm <sup>2</sup> /s)
$L$	total length of adsorption train (cm)

$n$	total number of transfer units in adsorption train [ $= 15(1 - \varepsilon)D_e L / ur_p^2$ ]
$N_c$	number of columns in series in the adsorption train
$q$	adsorbed concentration ( $\text{mg}/\text{cm}^3$ )
$\bar{q}$	concentration averaged over particle volume ( $\text{mg}/\text{cm}^3$ )
$q_F$	adsorbed concentration at equilibrium with feed ( $\text{mg}/\text{cm}^3$ )
$q_m$	monolayer adsorption capacity in Langmuir model ( $\text{mg}/\text{cm}^3$ )
$r$	radial coordinate (cm)
$r_p$	particle radius (cm)
$R$	isotherm parameter defined as $R = 1/(1 + bC_F)$
$u$	superficial velocity (cm/s)
$t$	time (s)
$t_{cycle}$	total time required for a column to cycle through the adsorption train (s)
$t_{reg}$	time required for elution, regeneration, and cleaning (s)
$t_{switch}$	switch time (s)
$x$	dimensionless pore fluid concentration ( $= c/C_F$ )
$X$	dimensionless fluid phase concentration ( $= C/C_F$ )
$Y$	dimensionless concentration in particle ( $= q/q_F$ )
$z$	axial coordinate

### Greek Symbols

$\varepsilon$	extraparticle porosity
$\varepsilon_p$	intraparticle porosity
$\Lambda$	partition ratio [ $= (1 - \varepsilon)q_F/C_F$ ]
$\rho$	dimensionless radial coordinate ( $= r/r_p$ )
$\tau$	dimensionless time ( $= ut/\Lambda L$ )
$\tau_p$	dimensionless total cycle time ( $= ut_{cycle}/\Lambda L$ )
$\zeta$	dimensionless axial coordinate ( $= z/L$ )

### REFERENCES

- Ruthven, D.M. (1984) *Principles of Adsorption and Adsorption Processes*; Wiley: New York, 394–396.
- Neretnieks, I. (1975) A simplified theoretical comparison of periodic and countercurrent adsorption. *Chem. Ing. Technik*, 47: 773.
- Svedberg, U.G. (1976) Numerical solution of multicolumn adsorption processes under periodic countercurrent operation. *Chem. Eng. Sci.*, 31: 345.
- Liapis, A.I.; Rippin, D.W.T. (1979) The simulation of binary adsorption in continuous countercurrent operation and a comparison with other operating modes. *AICHE J.*, 25: 455.
- Ortlib, H.-J.; Bunke, G.; Gelbin, D. (1981) Separation efficiency in the cyclic steady state for periodic countercurrent adsorption. *Chem. Eng. Sci.*, 36: 1009.
- Carta, G.; Pigford, R.L. (1986) Periodic countercurrent operation of sorption processes applied to water desalination with thermally regenerable ion-exchange resins. *Ind. Eng. Chem. Fundam.*, 25: 677.
- Liu, P.D.; Pigford, R.L. (1987) Preparative Separation of Proteins by Periodic Countercurrent Sorption. Paper presented at the AIChE Spring National meeting, Houston, TX, USA.
- Arve, B.H.; Liapis, A.I. (1988) Biospecific adsorption in fixed and periodic countercurrent beds. *Biotechnol. Bioeng.*, 32: 616.
- Holzer, M.; Osuna-Sanchez, H.; David, L. (2008) Multicolumn chromatography – A new approach to relieving capacity bottlenecks for downstream processing efficiency. *Bioprocess International*, September 2008, p. 74.
- Carta, G.; Ubiera, A.R.; Pabst, T.M. (2005) Protein mass transfer kinetics in ion exchange media: Measurements and interpretations. *Chem. Eng. Technol.*, 28: 1252.
- LeVan, M.D.; Carta, G. (2007) Adsorption and Ion Exchange. In: *Perry's Chemical Engineers' Handbook*, 8th ed., Section 16; Green, D.W. ed.; McGraw-Hill: New York.
- Bankston, T.E.; Stone, M.C.; Carta, G. (2008) Theory and applications of refractive index based optical microscopy to measure protein mass transfer in spherical adsorbent particles. *J. Chromatogr. A*, 1188: 242.
- Cooper, R.S.; Liberman, D.A. (1970) Fixed bed adsorption kinetics with pore diffusion control. *Ind. Eng. Chem. Fundam.*, 9: 620.
- Perez-Almodovar, E. X. (2009) Characterization of a new protein A adsorbent based on macroporous hydrophilic polymer beads. M.S. Thesis, University of Virginia, Charlottesville, Virginia.